Design and simulation of a wire position monitor for cryogenic systems in an ADS linac

ZHU Hong-Yan(朱洪岩)[1)] DONG Lan(董岚) LI Bo(李波)

Institute of High Energy Physics, Chinese Academy of Science, Beijing 100049, China

Abstract: This paper introduces the design and simulation of a Wire Position Monitor (WPM) used in the cryogenic system of an Accelerator Driven System (ADS). The WPM is designed to monitor the contraction of cold masses during the cooling-down operation. In this paper, POISSON-2D electrostatic field software is used to calculate the best characteristic impedance for the WPM. Furthermore, the time domain signal of different end structures is theoretically analyzed and simulated. The coupling of electrodes and the influence of signal carrier size, which may influence the induced signal, are also discussed. Finally, the linearity of the induced voltage and the sensitivity of the WPM are analyzed. The time domain simulation results are consistent with the theoretical analysis. The influences of the coupling and carrier size are very small, and the linearity of the normalized voltage is good within $r/2$.

Key words: wire position monitor, impedance match, coupling, CST simulation

PACS: 29.20.Ej **DOI:** 10.1088/1674-1137/38/8/087001

1 Introduction

IHEP is developing an Accelerator Driven System (ADS) with a working temperature of 2 K (temperature of liquid helium (LHe)). Each cryostat has 6 superconducting cavities and 5 superconducting magnets. Alignment will first be carried out at room temperature. When the temperature is dropped to 2 K, the positional error of the cavities and magnets must remain within ±0.1 mm after contraction.

Conventional alignment methods cannot work in this situation. There is no proven method or actual experience of collimation of facilities within a cryostat at any domestic accelerator centers.

In DESY's collimation plan [4], a Wire Position Monitor (WPM) is designed to monitor the contraction of cold masses during the cooling-down operation. A signal carrier wire passes through the center of the WPM; the other end is fixed outside the system. The WPM is attached to the cavities and magnets; it will move around with the system during contraction. The induced voltage of the microstrips will change with this relative movement; the wire position can then be obtained from the induced voltage on the four microstrips.

2 Principles of wire position monitor

The principle of the WPM is similar to that of a Beam Position Monitor (BPM). Four electrodes generate induced voltage when an RF signal passes through the center. We can get the X, Y position from the voltage on opposing pairs of strips. Based on the Mirror Current principle and on the electrodes being close to the WPM body, we can get the wire's normalized position [1]:

$$D_X = \frac{V_{\rm B}-V_{\rm D}}{V_{\rm B}+V_{\rm D}} = \frac{4\sin(\phi/2)}{\phi/2}\cdot\frac{x}{2b} + \frac{2\sin(3\phi/2)}{3\phi/2}\cdot\left[\left(\frac{x}{b}\right)^3+\frac{3xy^2}{b^3}\right]. \quad (1)$$

$$D_Y = \frac{V_{\rm A}-V_{\rm C}}{V_{\rm A}+V_{\rm C}} = \frac{4\sin(\phi/2)}{\phi/2}\cdot\frac{y}{2b} + \frac{2\sin(3\phi/2)}{3\phi/2}\cdot\left[\left(\frac{y}{b}\right)^3+\frac{3yx^2}{b^3}\right]. \quad (2)$$

In the formula, b is the inner radius of the WPM, ϕ is the flare angle of the strip, x and y are the distance away from the center in each direction.

From the above two expressions, we can tell that the normalized position is related to higher terms of distance away from the center, so the linearity is not constant [2].

3 Design and simulation of the wire position monitor

The design presented here uses a microstrip structure. In order not to interfere with other high frequencies in the cryostat, we choose a 215 MHz RF signal

Received 9 October 2013, Revised 25 January 2014

1) E-mail: zhuhy@ihep.ac.cn

as an excitation source. The parameters that will affect the character of the WPM are: characteristic impedance, end structure, coupling between strips and carrier size. Each of these is discussed in detail below.

3.1 Characteristic impedance

The input impedance of the external processing circuit is 50 Ω, so the characteristic impedance of the WPM should also be 50 Ω, to prevent signal reflection. The four-strip structure generates four sensing modes: sum mode, horizontal dipole mode, vertical dipole mode and quadrupled mode. The characteristic impedance under each mode is different. Because electrostatic field distribution of the two dipole modes is symmetrical, their impedance is the same. The best match condition is [1]:

$$\sqrt{Z_{\rm sum}Z_{\rm quad}}=Z_{\rm dipole}=50\ \Omega. \tag{3}$$

The structure of the WPM is calculated with the 2D electrostatic field solver POISSON. We can achieve the best match by adjusting the inner diameter, strip size and distance between strip and center. The simulated electrostatic fields of the four modes are shown in Fig. 1 below.

3.2 End structure

There are three possible end structures for the WPM: shorted structure, open structure and matched impedance structure. Different structures will cause different signal patterns at the readout end.

The reflection parameter of a radio frequency circuit [3] is:

$$\rho=\frac{Z_2-Z_1}{Z_2+Z_1}, \tag{4}$$

where Z_2 is the characteristic impedance of the WPM and Z_1 is the load impedance.

For a shorted structure, Z_1=0, ρ=1, all the signal will be reflected.

If the load impedance is matched, $Z_1=Z_2$, ρ=0, there is no reflection.

The schematic for signal generation of the matched impedance structure is shown in Fig. 2.

At $t1$=0, the signal passes the upstream port 1, where wall current is divided into equal halves, due to the equal impedance $Z_0=Z_2$=50 Ω, $t2=1/2\times L/c$.

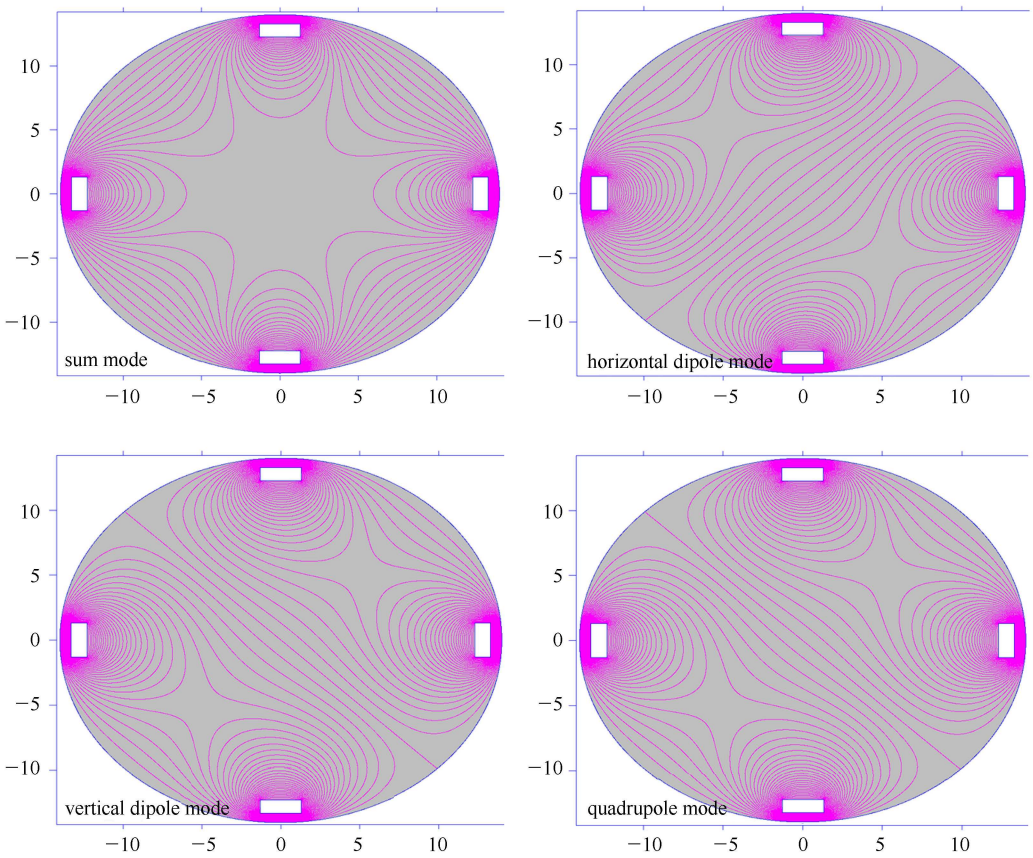

Fig. 1. Electrostatic field distribution of the four WPM modes.

At $t3=L/c$, the signal reaches the downstream port 2, where the image charge will generate an equal amplitude but opposite sign wall current as at port 1, and will also be divided into equal halves because of equal impedance $Z_0=Z_2=50$. Half of the signal will therefore cancel the initial signal generated at port 1. The other half will travel backwards to port 1.

The schematic for signal generation of the shorted structure is shown in Fig. 3.

At $t1=0$, the generated wall current will be divided into equal halves as in the matched impedance structure.

At $t3=L/c$, the image charge will also generate an equal amplitude but opposite sign wall current.

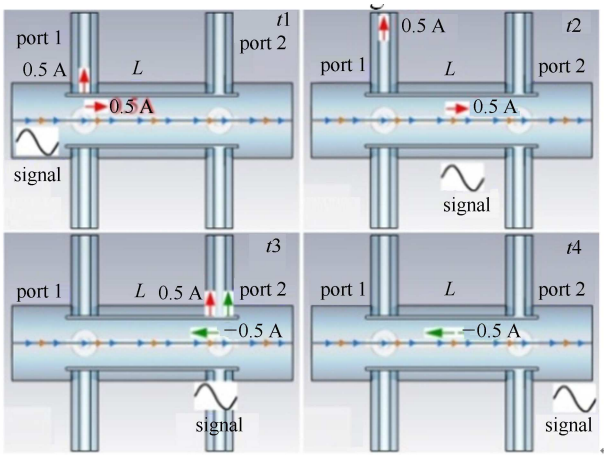

Fig. 2. Signal generation for the matched impedance structure.

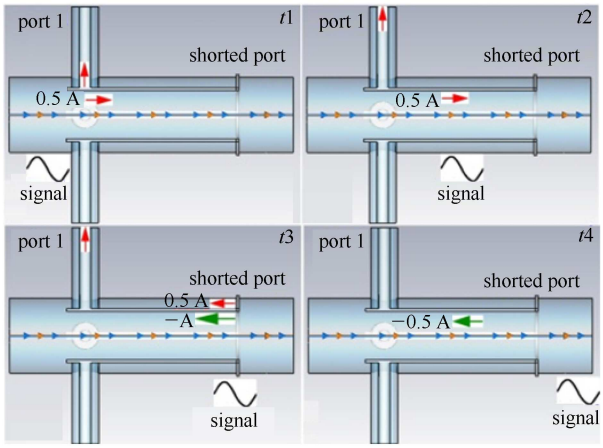

Fig. 3. Signal generation of shorted structure.

Although the travel direction of the initial half of the signal generated at port 1 is different, it will be canceled by the signal generated at port 2, so the backward signal is the same.

The final signal at port 1 should therefore be of the same form as for the matched impedance structure [7].

The simulation results in the time domain are shown in Figs. 4, 5. The excitation source is a sinusoidal signal with amplitude of 1 V. The unit of the simulated voltage signal is V in all the time domain figures, the same unit as the excitation.

The simulated signal of the two structures is basically the same, consistent with the analysis.

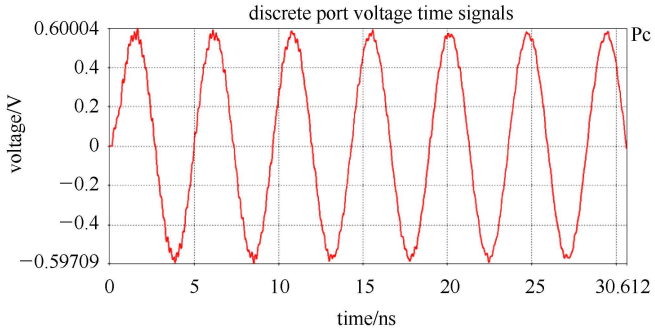

Fig. 4. Simulation result of shorted structure.

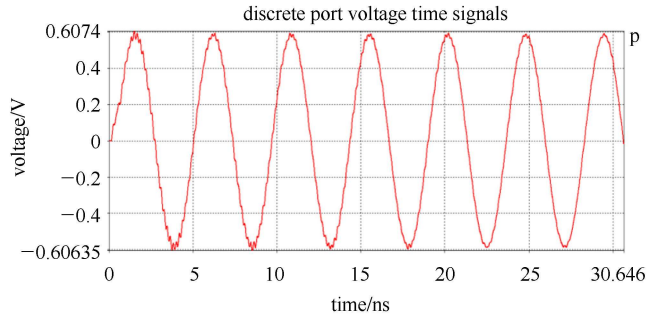

Fig. 5. Simulation result of matched impedance structure.

In this paper, we apply the matched impedance structure.

3.3 Coupling between microstrips.

The coupling between microstrips may affect the WPM probe's sensitivity and linearity [2, 5]. If coupling is taken into consideration, the normalized wire position calculated by the difference-over-sum method $(R-L)/(R+L)$ will be:

$$S_{\Delta-\Sigma}=\frac{(I_{\rm R}-I_{\rm L})(k_0-k_2)}{(I_{\rm R}+I_{\rm L})(k_0+2k_1+k_2)}=S_0\cdot K, \tag{5}$$

where k_1, k_2 are the coupling coefficients of adjacent and opposite microstrips, and S_0 is the sensitivity without coupling. K is a correction coefficient, described by:

$$K=\frac{1-k_2/k_0}{1+2k_1/k_0+k_2/k_0}. \tag{6}$$

From the above expression, we can tell that the correction coefficient is related only to the coupling coefficient parameters, irrespective of the wire position. It is a constant for any given structure.

The normalized wire position, calculated by the logarithmic ratio $\ln(R/L)$ is:

$$S_{\ln}=\ln\left(\frac{I_{\rm P}}{I_{\rm L}}\right)+\ln\left(\frac{(k_0+k_1)+(k_2+k_1)\dfrac{I_{\rm L}}{I_{\rm R}}}{(k_0+k_1)+(k_2+k_1)\dfrac{I_{\rm R}}{I_{\rm L}}}\right). \quad (7)$$

The sensitivity is related to the coupling coefficient parameters as well as with wire position. It is not a constant, so it will affect linearity in this method.

We can add an isolator to deduce the coupling strength, as shown by the model in Fig. 6. The coupling coefficients of different isolators are shown in Fig. 7

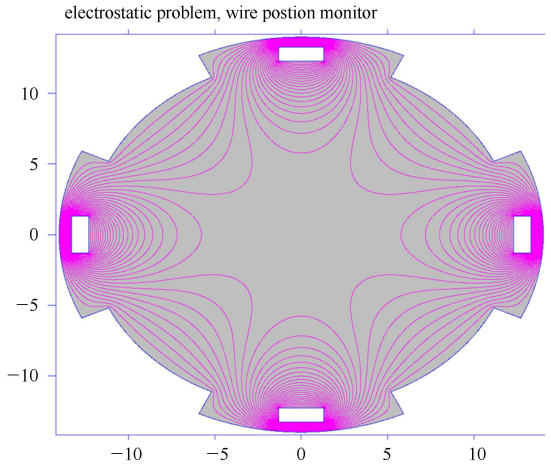

Fig. 6. Isolator.

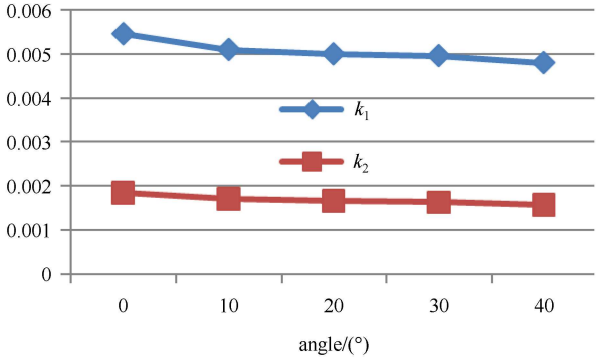

Fig. 7. Coupling coefficients of isolators.

From Fig. 7 we can tell that the coupling coefficients for both opposite and adjacent electrodes are very small. The corrected coefficient of a non-isolator structure is 0.982; the coefficient with an isolator at 40° is 0.984. The improvement is not significant. As the structure without an isolator is much simpler, we choose a non-isolator structure.

3.4 Carrier size

Considering the signal attenuation and strength under LHe temperature, we choose heat treated CuBe as the signal carrier. In this section, we present the results of simulations with two diameters of wire to see whether carrier size affects the induced voltage. Simulation results are shown in Fig. 8.

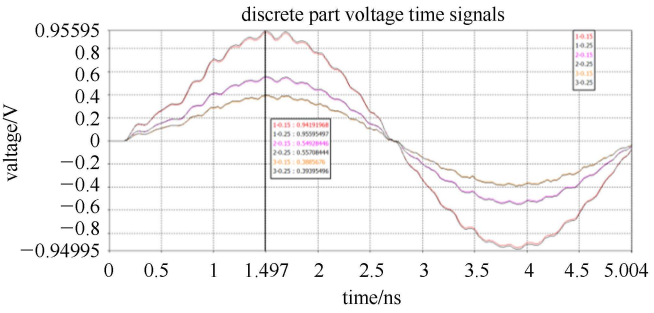

Fig. 8. Time domain signal for different carrier sizes.

From the simulation results, we can see there is no significant difference in the amplitudes of the induced voltage. The carrier in the simulation model is a perfect conductor. In actual use, there will be a certain attenuation within the 6 m transmission distance. Also, the impedance of the cylinder conductor decreases with the increase in diameter. Considering the attenuation, strength and sag, we choose 0.5 mm BeCu as the carrier.

3.5 Sensitivity and linearity of induced signal.

The expression for sensitivity [6] is:

$$\delta r=\frac{\sqrt{2}\pi^2 b}{I_{\rm b}Z_2}V_{\rm N}, \quad (8)$$

where $I_{\rm b}$ is the current on the carrier, $V_{\rm N}$ is the electric thermal noise level. If $I_{\rm b}$=20 mA, the theoretical sensitivity is 1.265 μm, which can satisfy the measurement requirement quite well.

Figure 9 shows the voltage on all four electrodes in the time domain for the case where the wire is displaced from the center by ($x=b/3$). In order to simulate relative

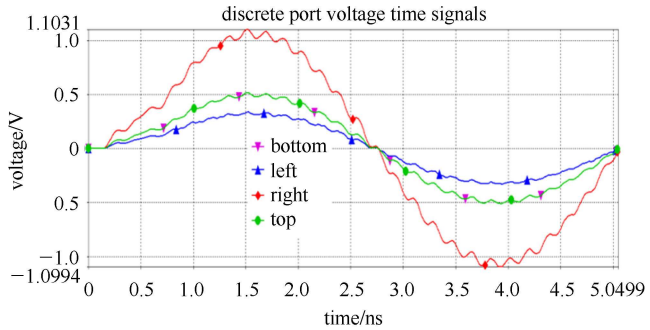

Fig. 9. Time domain signals when the four electrodes are displaced by $b/3$.

Table 1. Induced signal and normalized position.

wire position	@215 MHz @MWS					
mm	V_R/V	V_T/V	V_L/V	V_B/V	D_X	L_X
0	0.4112	0.4112	0.4112	0.4112	0.0001	0.0001
0.5	0.4383	0.4083	0.3811	0.4083	0.0698	0.0607
1	0.4766	0.4137	0.3581	0.4137	0.1419	0.1241
1.5	0.5141	0.4128	0.3331	0.4128	0.2137	0.1886
2	0.546	0.3967	0.3073	0.3967	0.2797	0.2496
2.5	0.5995	0.3931	0.2899	0.3931	0.3481	0.3155
3	0.6468	0.3782	0.2685	0.3782	0.4133	0.3818
3.5	0.6887	0.3624	0.2452	0.3624	0.475	0.4486
4	0.752	0.3512	0.2288	0.3512	0.5335	0.5168
4.5	0.8266	0.3372	0.2128	0.3372	0.5906	0.5894
5	0.8875	0.3232	0.1984	0.3232	0.6346	0.6506
5.5	0.9639	0.305	0.1821	0.305	0.6823	0.7238
6	1.0667	0.2894	0.1681	0.2894	0.7278	0.8025

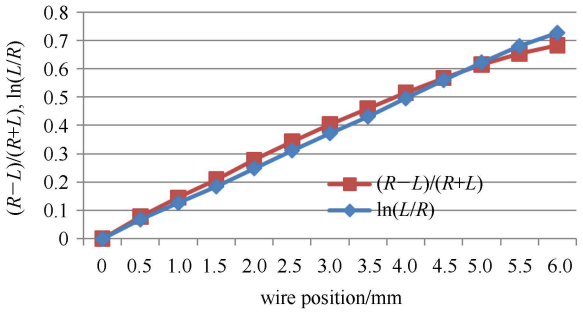

Fig. 10. Normalized position calculated by $(R-L)/(R+L)$ and $\ln(R/L)$ within 6 mm.

movement, we move the wire in steps of 0.5 mm and get the corresponding induced signal for each step, then calculate the normalized position.

The simulation results are shown in Table 1. V_L, V_T, V_R, V_B are the RMS induced voltage on the left, top, right and bottom electrodes of the WPM respectively. D_X is the normalized position calculated by the difference-over-sum $(R-L)/(R+L)$, while L_X is by log ratio $\ln(R/L)$. The inner radius of the WPM is 14 mm. Fig. 10 shows the linearity of the normalized position calculated by the difference-over-sum method and the log ratio method. From Fig. 10, we can tell that the linearity calculated by the log ratio is better than the difference-over-sum method. Good linearity will simplify the follow-up application.

4 Summary

In this paper, under the best match condition achieved by optimization of the 2D electrostatic field solver POISSON, we discussed several factors which may affect a WPM's performance, including end structure, coupling and carrier size, and determined the final design parameters. We then analyzed the sensitivity and linearity of the WPM. The linearity calculated by the log ratio method is better than the difference-over-sum method, and the theoretical sensitivity can also meet the requirements of the experiment.

References

1 Gassner G. Experience Report with the Alignment Diagnostic System. SLAC Stanford. 2010
2 YUAN Ren-Xian. Study and Application of Beam Position Measurement. Beijing. IHEP. 2004
3 Deibele C. Synthesis and Considerations for OptimallyMatching to a Beam Position Monitor Circuit Impedance, SNS-NOTE-DIAG-31
4 Bosotti A, Pagani C, Varisco G. On Line Monitoring of the TTF Cryostats Cold Mass with Wire Position Monitors. INFN/TC– 00/02 (Mar 17, 2000)
5 Giove D, Bosotti A, Pagani C. A Wire Position Monitor (WPM) System to Control the Cold Mass Movements Inside the TRF Cryomodule. Particle Accelerator Conference. 1997
6 Shafer R E. Beam Position Monitor Sensitivity for Low-beta Beams. AIP Conference Proceedings 319. New York: American Institute of Physics, 1994. 303–308
7 Peter Forck, PiotrKowina, Dmitry Liakin. Beam position monitor. Helmholtz Centre for Heavy Ion Research GSI. Germany. 2008